IRAQI JOURNAL OF MATERIALS
Volume (5) Issue (2) April-June 2026, pp. 59-66
Published and Sponsored by American Quality for Scientific Publishing, Inc. (AQSP)

Characterization of Periodic Ag/Al_2O_3/SiO_2/Si Multilayer Structures by Spectroscopic Ellipsometry

Maher S. Hanafy, Bahaa C. Hiad*, Eslam A.H. Elsharnoby

Department of Physics, Faculty of Science, Suhag University, Suhag, EGYPT
** Corresponding author email: bahaa.chiad@gmail.com*

Abstract
In this work, multilayer structures based on consecutive thin films of silver (Ag) and alumina (Al_2O_3) were grown on silicon substrates by RF reactive sputtering technique. With a layer period containing consecutive Ag and Al_2O_3 films, the number of these periods was varied to introduce their effects on the optical characteristics of the fabricated structures. The spectroscopic ellipsometry was carried out on these structures to determine the ellipsometric parameters (amplitude ratio Ψ and phase shift difference Δ) as functions of incident light wavelength for three different incidence angles (60°, 70°, and 80°). Results showed that the larger number of periods resulted in a higher sensitivity to the incidence angle by the multilayer structure, which is very crucial for practical applications such as optical filters and photonic sensors as the thickness and structure of these layers are controlled to achieve certain optical response within a desired wavelength ranges.

Keywords: Ellipsometry; Multilayer structures; Amplitude ratio; Phase shift difference
Received: November 2025; **Revised:** January 2026; **Accepted:** February 2026; **Published:** April 2026

1. Introduction

Metamaterials represent a real revolution in modern optics as their optical properties exceed the limits of natural materials. The original idea of the metamaterials belongs to the theoretical fundamentals established by Veselago in 1968 who assumed the existence of materials with negative electrical permittivity (ε) and magnetic permeability (μ) at the same time [1-3]. Among these materials, hyperbolic metamaterials (HMMs) are featured as extraordinarily efficient and promising materials due to their unique dynamic structure allowing them to control light beyond the diffraction limit [4]. The HMMs are described by their monoaxial anisotropic properties as they have tensorial permittivity, in which the sign of the component parallel to the surface ($\varepsilon_{||}$) is reversed to the sign of the component normal to the surface ($\varepsilon_{\perp}$). This is responsible of the formation of isofrequency surface as an open hyperboloid instead of closed ellipsoid, which is common in the conventional materials [5,6]. According to the geometry of the equivalent surfaces, unique optical properties are resulted, such as the possibility to support theoretically-unlimited large wave vectors. This leads to interesting physical phenomena like spontaneous emission enhancement. As well, the possibility to achieve super-resolution imaging, which exceeds the conventional diffraction limit of light [7]. The HMMs are classified into two main types. In the first type, $\varepsilon_{||}>0$ and $\varepsilon_{\perp}<0$, while in the second type, $\varepsilon_{||}<0$ and $\varepsilon_{\perp}>0$. These types show different characteristics of propagation and interaction with light [8-10].

The most common practical method to achieve these properties in the optical range is the preparation of consecutive thin films from metallic and dielectric layers with a condition that the layer thickness is reasonably smaller than the incident light wavelength in order to behave as an optically-active homogeneous medium according to the effective medium theory (EMT). For example, the Ag/Al_2O_3 system was widely investigated as basic and typical model to achieve this behavior. However, the transition from simple multilayer structure to a real HMM is not simultaneous as it depends on the correlation of several basic design parameters [11-13]. The occurrence of transition from elliptical dispersion to hyperbolic dispersion requires precise understanding for the correlation of parameters like metallic layer thickness (h_m) and dielectric layer thickness (h_d) those together determine the fill fraction (Φ) of the metal in the structure [14,15]. Also, the wavelength at which this transition occurs (λ_{HMM}) fundamentally depends on this fill fraction as well as the optical properties of the components (ε_d and ε_m) [16]. Moreover, merely satisfaction of these requirements is not enough as a minimum number of periods in the layers should be reached in order the behavior of the effective medium becomes dominant and the properties of the HMM appear completely. Here, the main challenge facing the actual

preparation and wide practical employment of these materials is apparently the difficulties in determination and verification of design parameters accurately using available and effective characterization techniques [17-19].

Spectroscopic ellipsometry is a non-destructive and powerful optical technique to meet this challenge. In this technique, the variation in light polarization beyond reflection from sample surface is measured to precisely extract the optical properties and dielectric functions of the thin layers [20-22]. By analyzing the ellipsometric parameters (Ψ and Δ) over a wide wavelength range, the slight variations in the tensorial electrical permittivity ($\varepsilon_{||}$ and $\varepsilon_{\perp}$) can be distinguished, and hence the wavelength at which the material's behavior converts from a system to another accurately can be determined [23]. The ellipsometric parameters (Ψ and Δ) are correlated by the following equation for complex reflectance ratio (ρ) [24]:

$$\rho = \frac{r_p}{rs} = tan(\Psi)e^{i\Delta} \quad (1)$$

With

$$tan(\Psi) = \left|\frac{r_p}{rs}\right| \qquad 0° \leq \Psi \leq 90° \quad (2)$$

where Ψ is the amplitude ratio between the p-polarized and s-polarized light after reflection, r_p and r_s are the complex reflection coefficients for light polarized parallel and normal, respectively, to the plane of incidence, and Δ is the phase shift difference between the p and s components, where 0°≤Δ≤180°

The capability of ellipsometry to correlate the theoretical modelling – based on EMT theory and transfer matrix charts method (TMM) – to the experimental measurements makes it an optimum methodology to create practical design charts. Such charts may provide clear instructions for researchers and manufacturers and enable them to determine the optimum parameters to synthesize HMMs with previously-determined properties. This may prepare to extend the employment of these materials from laboratories to real advanced applications such as quantum optics, sensing, and photonic integrated circuits.

2. Experimental Part

The multilayer structure shown in Fig. (1) was fabricated in this work by RF reactive sputtering technique. This structure contains of four main regions, substrate (silicon wafer), native oxide layer (SiO_2 thin film), consecutive metal/dielectric layers (Ag/Al_2O_3), and finally, protective layer (Al_2O_3 thin film). The advanced RF reactive sputtering technique provides precise control at the atomic scale of the thin film structure and thickness. The fabrication process was started by strictly cleaning a single-crystalline silicon wafer to remove any organic contaminations or tiny particles may affect the adhesion and growth of the deposited layers. The wafer was rinsed in a solution containing acetone, ethanol, and deionized water with mixing ratio of (1:1:2) in an ultrasonic bath, then dried with nitrogen to ensure a completely clean surface before transferred to the deposition vacuum chamber. This chamber was initially evacuated down to 10^{-6} torr to remove residual water vapor and gases from the deposition chamber. Figure (2) shows the RF sputtering system used in this work.

The substrate's temperature was controlled during deposition by an electric heater connected to the substrate inside the chamber and supplied by electrical power from a power supply outside the chamber. This temperature control is very necessary to avoid thermal stress. The deposition process was carried out at room temperature without heating of the substrate to achieve the required stability of the optical properties of the deposited layers. Using RF power is crucial when the Al_2O_3 thin films are deposited in order to prevent the charge accumulation on the surface of dielectric targets. To deposit silver (Ag) thin film, a highly pure (99.99%) silver target was sputtered in existence of argon gas at 13.56 MHz, whereas the Al_2O_3 thin film was deposited by sputtering highly pure (99.99%) aluminum target in existence of oxygen in the gas mixture ($Ar:O_2$) with mixing ratio of 1:1. This ratio could be precisely controlled throughout the flow rates of both gases into an external mixer before the mixture was pumped into the deposition chamber. Fine control of RF power, gas mixture pressure and mixing ratio is crucial to ensure the deposition of approximately stoichiometric Al_2O_3 thin films free of oxygen vacancies that may cause undesired optical absorption.

In order to achieve the periodic structure, a 100nm-thick layer of Al_2O_3 film was deposited on the SiO_2 layer, then a 100nm-thick Ag film was deposited. These two thin films form a single period in the periodic structure. This period was repeated to prepare N periods before a 80nm-thick Al_2O_3 film was deposited as a protective layer. The film thickness was determined by deposition time according to the deposition rates of sputtered materials. The silicon substrate was rotated during deposition to ensure homogeneous film thickness as much as possible. As well, a dc biasing voltage of 5 V was applied to

 ISSN (print) 2958-8960 (online) 3006-6042 Printed in IRAQ

IRAQI JOURNAL OF MATERIALS
Volume (5) Issue (2) April-June 2026, pp. 59-66
Published and Sponsored by American Quality for Scientific Publishing, Inc. (AQSP)

the substrate to enhance the characteristic of the deposited films, such as film density, adhesion, and oxygen contamination, especially when Ag films were deposited. After the completion of deposition process, the multilayer sample was kept inside the chamber before transferred to the ellipsometry experimental setup to measure its optical properties.

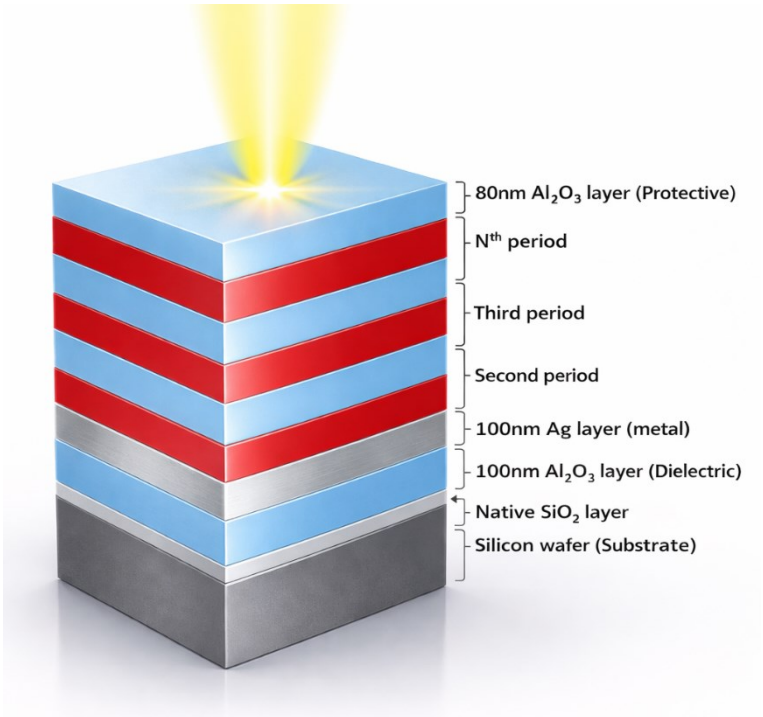

Fig. (1) Schematic diagram of the HMM structures fabricated in this work

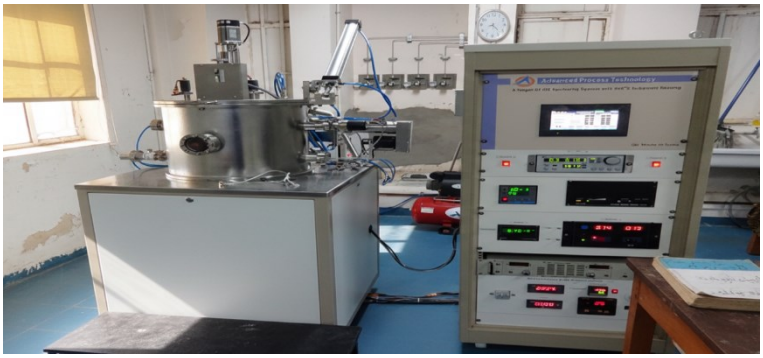

Fig. (2) RF sputtering system used in this work

3. Results and Discussion

Figure (3) shows the variation of the amplitude ratio (Ψ) as an ellipsometric parameter with incident light wavelength for three different incidence angles (60°, 70°, and 80°) for the fabricated structure based on one period of Ag and Al_2O_3 films. The values of Ψ follows a clear oscillating behavior over the range from 27° to 43° depending on the incidence angle and light wavelength. At shorter wavelengths (300-500nm) the incidence angle of 60° produce the highest values of Ψ with gradual decrease with increasing wavelength. Therefore, the three curves are converging. Within wavelength range of 500-900nm, the values of Ψ gradually decrease for all incidence angles to reach its minimum of about 27° at 900nm for incidence angle of 80°. In the wavelength region longer than 900nm, the values of Ψ are approximately stable within the range of 27°-37° with apparent differences with respect to the incidence angle. An interesting behavior is observed when the Ψ values gradually increases again. This oscillating behavior reveals a complex interference of light within the multilayer structure. This behavior is

IRAQI JOURNAL OF MATERIALS
Volume (5) Issue (2) April-June 2026, pp. 59-66
Published and Sponsored by American Quality for Scientific Publishing, Inc. (AQSP)

sufficiently affected by the properties of the dielectric Al_2O_3 and metallic Ag layers. The variations in the slope, maxima, and minima of the three curves are related to the phenomena of constructive and destructive interference inside the thin layers [25,26]. As well, the convergence of these curves at specific wavelengths refers to optical balance points where the effect of incidence angle is slight [27]. These results are crucial to understand the optical characteristics of multilayer structures and their applications in designing optical filters and photonic sensors as the thickness and structure of these layers are controlled to achieve certain optical response within a desired wavelength ranges.

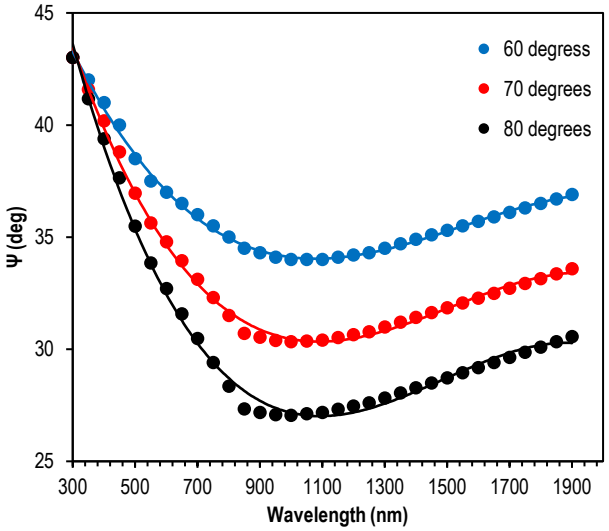

Fig. (3) Variation of electrical resistivity with graphene content

Figure (4) shows the variation of the phase shift difference (Δ) as an ellipsometric parameter with incident light wavelength for three different incidence angles (60°, 70°, and 80°) for the fabricated structure based on one period of Ag and Al_2O_3 films. The values of Δ shows continuous increase with wavelength starting from relatively low values (40°-70°) at 300nm to reach very high values (>150°) at 1900nm. An approximately linear relationship between Δ and λ can be observed in the wavelength range of 700-1900nm. The effect of incidence angle is also observed as the smaller angle (60°) produces the higher values of Δ, which confirms the sensitivity of the ellipsometric parameters to the light incidence angle in the multilayer structures. The continuous increase in Δ refers to a gradual variation in the phase difference between the normal and parallel components of the reflected light those relate to the complex interference characteristics within the thin layers. The semi-linear relationship between Δ and λ is very useful in practical applications because it allows an accurate calibration of the optical characteristics of the layers [28,29].

Figure (5) shows the variation of the amplitude ratio (Ψ) as an ellipsometric parameter with incident light wavelength for three different incidence angles (60°, 70°, and 80°) for the fabricated structure based on four periods of consecutive Ag and Al_2O_3 films. A distinct behavior shown by these curves highlights the increasing optical complexity with additional periods. In the wavelength range of 300-500nm, the value of Ψ is sharply increased from 22° to 35° for the incidence angle of 60° while larger incidence angles (70° and 80°) produce lower values of Ψ. A slow gradual increase is seen within 500-900nm range and a constant (saturated) behavior is observed at wavelength longer than 900nm (41.5°-43° for incidence angle of 60°, 33.2°-34.6° for 70°, and 23°-23.65° for 80°). This behavior indicates an important physical phenomenon expressing that the multilayer structure has reached an optical stability where the effect of wavelength variation on the amplitude ratio (Ψ) is slight [30]. This is attributed to the formation of stable interference modes within the periodic structure as the light waves achieve a phase balance after sufficient number of reflections between the layers. When compared to the one-period structure, the effect of periodic structure can be apparently observed in softening the oscillations and hence achieving better optical stability. Such characteristics make these structures optimum candidates for applications requiring constant or stable optical response over a wide spectral range due to the resulted high-reliable performance and accurate measurements [31,32].

IRAQI JOURNAL OF MATERIALS
Volume (5) Issue (2) April-June 2026, pp. 59-66
Published and Sponsored by American Quality for Scientific Publishing, Inc. (AQSP)

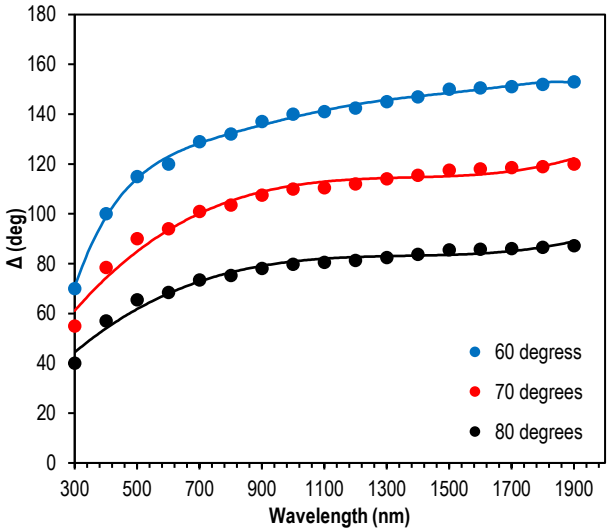

Fig. (4) Variation of electrical resistivity with graphene content

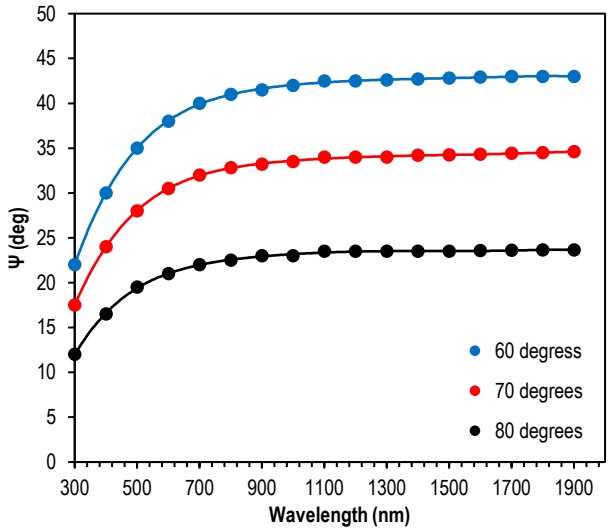

Fig. (5) Variation of electrical resistivity with graphene content

Figure (6) shows the variation of the phase shift difference (Δ) as an ellipsometric parameter with incident light wavelength for three different incidence angles (60°, 70°, and 80°) for the fabricated structure based on four periods of consecutive Ag and Al_2O_3 films. Initially, the value of Δ are decreasing in the region between 300 and 400 nm before rapidly increasing within the range of 400-900nm. After that, the increase in Δ becomes slower at wavelengths longer than 900nm. The effect of the incidence angle is apparent to confirm the sensitivity of the Δ measurement in the periodic multilayer structure. The approximately linear behavior within 900-1900nm may facilitate the modelling and expectation of the optical behavior of the structure. When compared to the one-period structure, an increase in the Δ values is observed (153° for one period and 158° for four periods) due to the effect of supported constructive interference.

Figure (7) shows the variation of the amplitude ratio (Ψ) as an ellipsometric parameter with incident light wavelength for three different incidence angles (60°, 70°, and 80°) for the fabricated structure based on seven periods of consecutive Ag and Al_2O_3 films. The curves in this figure show a modified mode due to the accumulative effect of increasing the number of periods on the optical characteristics. Again, these curves indicate a kind of saturation in the Ψ values since the multilayer structure is seen as a homogeneous optical medium with specific characteristics regardless the incident wavelength. Also, these curves confirm how the larger number of periods leads to enhance the optical stability and

reasonably decrease the oscillations. The stable values of Ψ may make these multilayers structures suitable for the applications of phase modulation at the near-infrared (NIR) wavelengths [34].

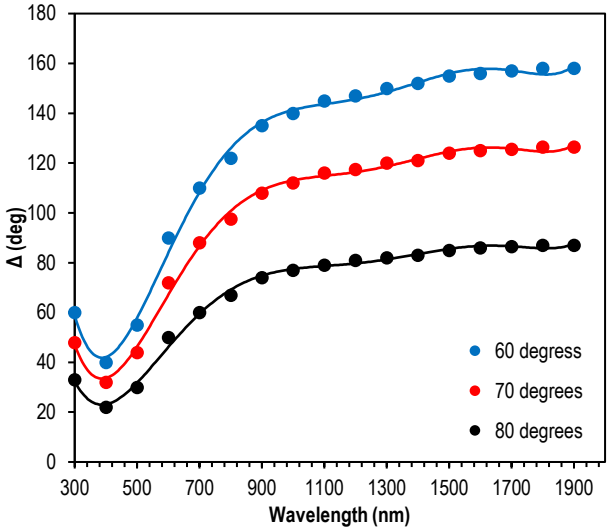

Fig. (6) Variation of electrical resistivity with graphene content

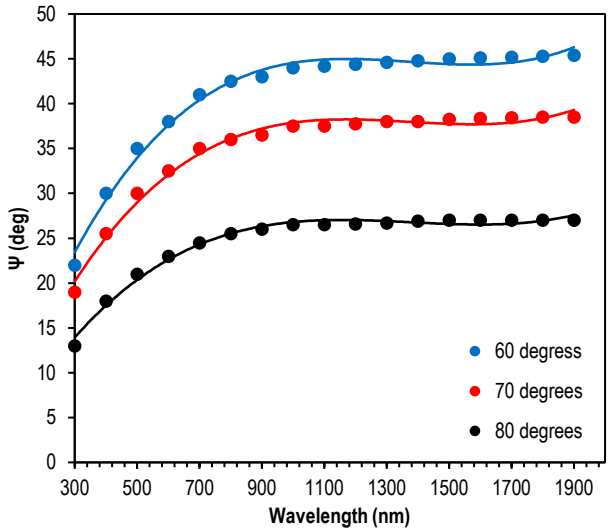

Fig. (7) Variation of electrical resistivity with graphene content

Figure (8) shows the variation of the phase shift difference (Δ) as an ellipsometric parameter with incident light wavelength for three different incidence angles (60°, 70°, and 80°) for the fabricated structure based on seven periods of consecutive Ag and Al_2O_3 films. With similar behavior shown in previous figures, a further confirmation is seen throughout this figure for the enhancement of optical characteristics of the multilayer structure due to increasing the number of multilayer periods to seven.

4. Conclusions

In concluding remarks, multilayer structures were successfully fabricated from consecutive periods of Ag/Al_2O_3 thin films on silicon substrates by RF reactive sputtering technique. The effect of increasing number of periods on the ellipsometric parameters of these structures was introduced as a conversion from oscillating to stable state in these parameters was observed as the structure behaved like a homogeneous medium. Such stable optical characteristics over a wide range of wavelengths (300-1900nm) make these multilayer structures optimum choice for optical and photonic applications requiring stable and reliable performance such as optical filters, photonic sensors, and phase modulators in the NIR region.

ISSN (print) 2958-8960 (online) 3006-6042

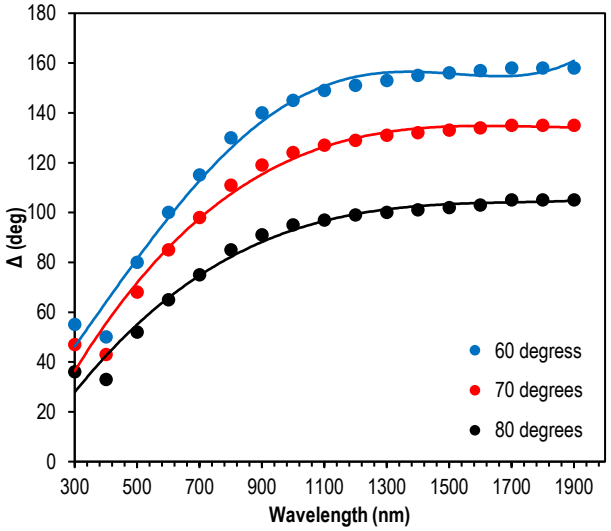

Fig. (8) Variation of electrical resistivity with graphene content

References

[1] C. Chen et al., "Piezoresistive behavior of epoxy-based nanocomposites near the percolation threshold", Carbon, 195 (2022) 200-215. 3333
[2] R. Lei et al., "Environment-adaptive design of multilayer optical structures for surface polariton excitation via dynamic multi-objective optimization", *Defence Technol.*, (2025), doi.org/10.1016/j.dt.2025.11.013.
[3] H. Chen et al., "(INVITED) Tungsten oxide films by radio-frequency magnetron sputtering for near-infrared photonics", *Opt. Mater.: X*, 12 (2021) 100093.
[4] J.-C. Chang et al., "Orthorhombic $Ta_{3-x}N_{5-y}O_y$ thin films grown by unbalanced magnetron sputtering: The role of oxygen on structure, composition, and optical properties", *Surf. Coat. Technol.*, 406 (2021) 126665.
[5] H.-Z. Gao et al., "Hyperbolic metamaterials based on multilayer Ag/TiN_xO_y structure for SPR refractive index sensors", *Opt. Laser Technol.*, 151 (2022) 108034.
[6] R.B. Tokas et al., "Study of reactive electron beam deposited tantalum penta oxide thin films with spectroscopic ellipsometry and atomic force microscopy", *Appl. Surf. Sci. Adv.*, 18 (2023) 100480.
[7] N. Malik et al., "Effect of post-annealing temperature and thickness on RF sputtered Al2O3 films for optoelectronic applications", *Result. Surf. Interfaces*, 19 (2025) 100480.
[8] D. Mukherjee et al., "Optimized sensing on gold nanoparticles created by graded-layer magnetron sputtering and annealing", *Sens. Actuat. B: Chem.*, 425 (2025) 136875.
[9] F. Huo et al., "Tantalum-doped tin oxide thin films using hollow cathode gas flow sputtering technology", *Heliyon*, 10(10) (2024) e30943.
[10] N. Zahra et al., "Enhanced measurement of smooth surface using the Spin Hall Effect of Light ellipsometry with near Brewster's angle incidence", *Measurement*, 263 (2026) 120163.
[11] W. Jin et al., "Thermochromic properties of ZnO/VO_2/ZnO films on soda lime silicate glass deposited by RF magnetron sputtering", *Ceram. Int.*, 49(7) (2023) 10437-10444.
[12] G.Zh. Moldabayeva et al., "Determination of the influence of variation in the number of layers in multilayer coatings on the inhibition of hydrogenation processes and thermal barrier characteristics", *RSC Adv.*, 15(28) (2025) 22941-22952.
[13] B. Putz et al., "In situ fragmentation of Al/Al_2O_3 multilayers on flexible substrates in biaxial tension", *Mater. Design*, 232 (2023) 112081.
[14] Y. Zhang, M.T. Phoo, and J.A. Zapien, "Ellipsometric characterization of magnetron sputtered metal-dielectric-metal (MDM) multilayers for Optical Vernier Scale biosensors with ultra-high sensitivity and large dynamic range", *Surf. Coat. Technol.*, 507 (2025) 132133.
[15] B.D. Igamov et al., "Comprehensive analysis of thickness-dependent structural, morphological, and optical properties of TiO_2 based thin films", *Result. Opt.*, 23 (2026) 100993.
[16] S.K. Honnali et al., "Epitaxial growth of TiZrNbTaN films without external heating by high-power impulse magnetron sputtering", *Surf. Coat. Technol.*, 495 (2025) 131583.
[17] D. De Luca et al., "Optical and structural properties of TaC thin films: Towards design of an efficient high temperature solar absorber coating", *Solar Energy*, 293 (2025) 113459.
[18] X.-X. Yang and F.-H. Lu, "Development of Ti-N-O-based multilayer low-emissivity coatings through air-based sputtering technique", *Appl. Surf. Sci. Adv.*, 30 (2025) 100902.
[19] A. Cheikh et al., "Tailoring structural and optical properties of Ta_2O_5 thin films via radio frequency magnetron sputtering for high-refractive index transparent materials", *J. Alloys Comp.*, 1040 (2025) 183273.
[20] C. Wheeler et al., "Multilayer W-doped vanadium dioxide thermal sensors with extended operation region", *iScience*, 28(6) (2025) 112528.
[21] C.-T. Lee et al., "Fabrication of a hot mirror using ITO-free electrochromic films", *Result. Opt.*, 16 (2024) 100735.
[22] N. Hegedüs et al., "Interpretation of hydrogen incorporation into radio frequency sputtered amorphous silicon based on Berg modelling", *Vacuum*, 202 (2022) 111164.

[23] D. Stock et al., "Development of direct current magnetron sputtered TiO_{2-x} thin films as buffer layers for copper indium gallium diselenide based solar cells, *Thin Solid Films*, 786 (20230 140115.
[24] A.S. Racz et al., "Evaluation of AES depth profiles with serious artefacts in C/W multilayers", *Appl. Surf. Sci.*, 582 (2022) 152385.
[25] P. Petrik, A.S. Racz, and M. Menyhard, "Complementary physicochemical analysis by ellipsometry and Auger spectroscopy of nano-sized protective coating layers", *Appl. Surf. Sci.*, 534 (2020) 147593.
[26] Ye.A. Kenzhin et al., "Determination of the efficiency of using multilayer CrN/MoN ceramic coatings for protection against hydrogen absorption and exposure to aggressive environments", *Open Ceram.*, 24 (2025) 100872.
[27] S. Meziani et al., "Mid-infrared integrated spectroscopic sensor based on chalcogenide glasses: Optical characterization and sensing applications", *Adv. Sens. Ener. Mater.*, 4(3) (2025) 100149.
[28] A. Elsafi et al., "Performance and durability of anti-soiling and anti-reflective coatings for photovoltaic systems in desert climates", *Solar Energy*, 293 (2025) 113446.
[29] L. Antognini et al., "Integration of thin n-type nc-Si:H layers in the window-multilayer stack of heterojunction solar cells", *Sol. Ener. Mater. Solar Cells*, 248 (2022) 111975.
[30] S. Ono et al., "Comparative study of deposition characteristics a-C:H films by plasma CVD using methane, acetylene, and cumene", *Diamond Relat. Mater.*, 157 (2025) 112468.
[31] A. Wittrock et al., "Determining the thickness of plane and curved coatings by Raman scattering combined with laser ablation", *Surf. Interfaces*, 77 (2025) 108016.
[32] V. Siller et al., "Safe extended-range cycling of $Li_4Ti_5O_{12}$-based anodes for ultra-high capacity thin-film batteries", *Mater. Today Energy*, 25 (2022) 100979.
[33] M.A. Zahid et al., "Improved optical and electrical properties for heterojunction solar cell using Al_2O_3/ITO double-layer anti-reflective coating", *Result. Phys.*, 28 (2021) 104640.
[34] L. Souqui et al., "MgH_2 thin films and nanowires deposited by CVD from a magnesium diamidodiboranate precursor", *Mater. Today Commun.*, 50 (2026) 114615.

 ISSN (print) 2958-8960 (online) 3006-6042 Printed in IRAQ